JOURNAL OF MATERIALS SCIENCE 26 (1991) 4369–4374

Characterization of rapidly solidified structures of Al–6Fe–3MM

C. S. SIVARAMAKRISHNAN, K. LAL, R. K. MAHANTI
National Metallurgical Laboratory, Jamshedpur-831 007, India

Rapidly solidified and processed Al–6Fe–3MM (MM stands for Misch Metal) has been studied for microstructural characterization through optical microscopy, transmission electron microscopy and X-ray diffraction analysis. It has been shown that the RS ribbons of this alloy could be consolidated and processed through extrusion, forging and hot rolling and that the microstructures are stable up to 300 °C.

1. Introduction
Rapidly solidified aluminium alloys are being studied extensively for applications in aircraft and engineering structures [1, 2]. It is well known that the conventional high strength ingot aluminium alloys of the 7××× and 2××× series are suitable only for applications upto about 180 °C as microstructural deterioration takes place due to precipitate coarsening above this temperature [3].

The attributes of RS (solidification rates $> 10^4$ K s^{-1}) such as extended solid solubility, refinement of grain size and dendrite arm spacing and metastable phase formation have been successfully exploited in introducing low diffusivity elements like Fe, V, Zr, Ce, Mo, Mn etc. into aluminium alloys [4]. Table I gives the data on the equilibrium solid solubilities and their extension due to rapid solidification [5, 6]. Apart from imparting high strength the fine precipitates in the RS materials (which result from appropriate heat treatment) also inhibit grain growth as also do not coarsen themselves due to low diffusivity of the alloying additions, making these alloys suitable for high temperature applications [7, 8].

For the present work of microstructural characterization Al–6Fe–3MM (MM stands for misch metal) has been chosen to take advantage of low diffusivity of Fe in aluminium and useful compound formation of Al–Fe–MM. The characterization is based on the results of optical microscopy, transmission electron microscopy and X-ray diffraction analysis.

2. Experimental procedures
Alloys as given in Table II were prepared in gas fired furnace using 99.8% Al, 99.9% Fe and misch metal (50% Ce, 40% La, 3% Fe, balance other rare earth) and cast into 75 mm diameter 500 mm high chill moulds. The ingots, after homogenization at 550 °C for 24 h, were scrap cut, remelted in electric resistance furnace, degassed with hexachloroethane and cast into 20 mm diameter rods for melt spinning either in Marko Materials 2M Model Melt Spinner or in a melt spinning unit fabricated in the laboratory. The 2M Model consisted of a variable speed motor (max. 3600 r.p.m.), vacuum chamber, induction unit, where the molten metal is ejected by argon pressure through a 0.3 mm orifice onto the rotating copper disc to get ribbons of about 70 μm thickness. The laboratory fabricated unit, on the other hand, consisted of a 300 mm diameter copper drum fitted to a 720 r.p.m. motor, where the molten metal was poured in a 3 mm bottom holed crucible and allowed to fall on the rotating (19 m s^{-1} linear speed) copper drum to get ribbons of about 200 μm thickness. The two units are shown in Fig. 1. The cooling rates in the latter unit was, obviously, lower compared to the former unit because of lower speed.

The melt spun ribbons were pulverized using a mortar and pestle in the present work and compacted at room temperature under a load of 20 tonne in a hydraulic press to 50 mm diameter slugs. The slugs were extruded in a 500 tonne extrusion press at 300 °C to 20 mm rods. The extruded rods were forged at 400 °C to 6 mm thickness and hot rolled at the same temperature to sheets of 4 mm thickness. The flow chart of the processing adopted in this work is given in Fig. 2.

Optical microscopy, transmission electron microscopy and X-ray diffraction analysis were done on the

TABLE I Solid solubility of Fe, Mn, Ce and Zr in aluminium

Element	Equilibrium solid solubility	Extended solid solubility due to RS	Increase in solid solubility due to RS (x)
Mn	0.70	9.0	13
Fe	0.025	4.0	160
Zr	0.08	3.0	38
Ce	0.01	1.9	190

TABLE II Aluminium alloys investigated in the present work

Alloy	Nominal composition (wt %)		
	Fe	Misch metal	Balance
1	6	–	Al
2	6	3	Al

0022–2461/91 $03.00 + .12

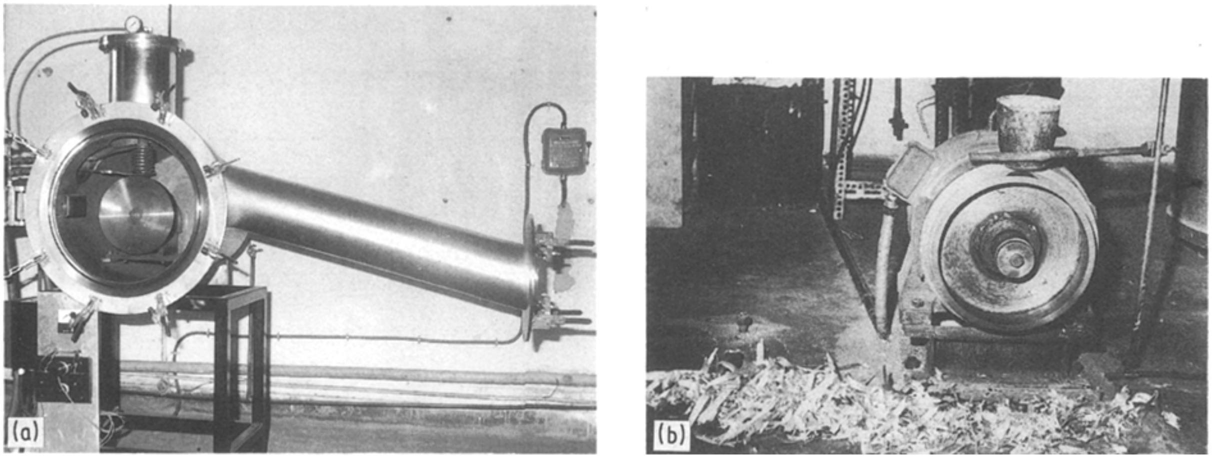

Figure 1 Melt spinning units for ribbon production: (a) 2M model Marko Materials Unit; (b) Laboratory fabricated unit.

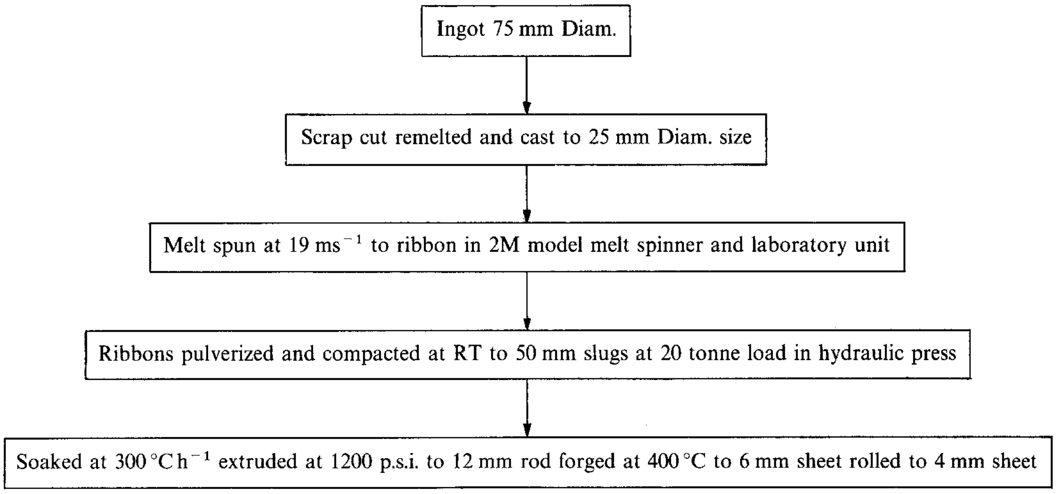

Figure 2 Flow chart of RS processing employed.

melt spun ribbon and the 4 mm sheets (extruded-forged-rolled). The sheets were also given heat treatment at 200 and 300 °C for 1 h and 3.5 h, respectively, to study the structural changes, if any.

Tensile tests were also carried out in a Hounsfield tensometer on the samples heat treated as above, as also on the as melt spun ribbon. In the case of as melt spun ribbon the tensile strength was determined on the ribbons of uniform cross-sections. Table III gives the tensile data.

3. Results and discussion

Fig. 3 shows the microstructures of the 25 mm diameter chill cast rods of Al–6Fe with and without addition of 3% MM. It may be noted that the basic matrix microstructural features are not changed with MM addition in the Al–6% Fe but the platelets of the intermetallic phase predominantly ($FeAl_3$) almost disappears in the latter.

The microstructure of the melt spun ribbon is shown in Fig. 4 which gives the details of the fine structure. The cooling rates in these experiments was $> 10^5$ K s^{-1} as measured from the secondary dendrite arm spacing from a number of locations of the ribbons. The average value was found to be ~ 2 µm. It is interesting to observe two distinct zones, A and B as reported by Jones [9]. Zone A structure, which is finer compared to Zone B and predominantly precipitate free forms near the wheel side of the ribbon, obviously due to the higher cooling rate than the air-side. It has been reported that a high degree of undercooling which results prior to nucleation on the wheel side [9] and kinetic effects of the solid–liquid interface resulting from partitionless solidification [10, 11] would be the causes for the formation of Zone A.

Towards the air side of the ribbon a coarse structure is seen (Zone B) and this has been attributed to low degree of undercooling or heterogeneous nucleation; low degree of undercooling resulting from reclescence [12]. The structure of Zone B is equiaxed dendritic type observed in constitutionally undercooled materials [13].

TABLE III Room temperature tensile strength of RS ribbon and RSP sheet of Al–6Fe–3MM

Alloy	UTS (MPa)		% Elongation 50 mm
	RS ribbon[a]	RSP sheet	gauge length
Al–6Fe–3MM	200	230–240	5

[a] Tensile strength of ribbons were determined on selected ribbons of uniform cross section.

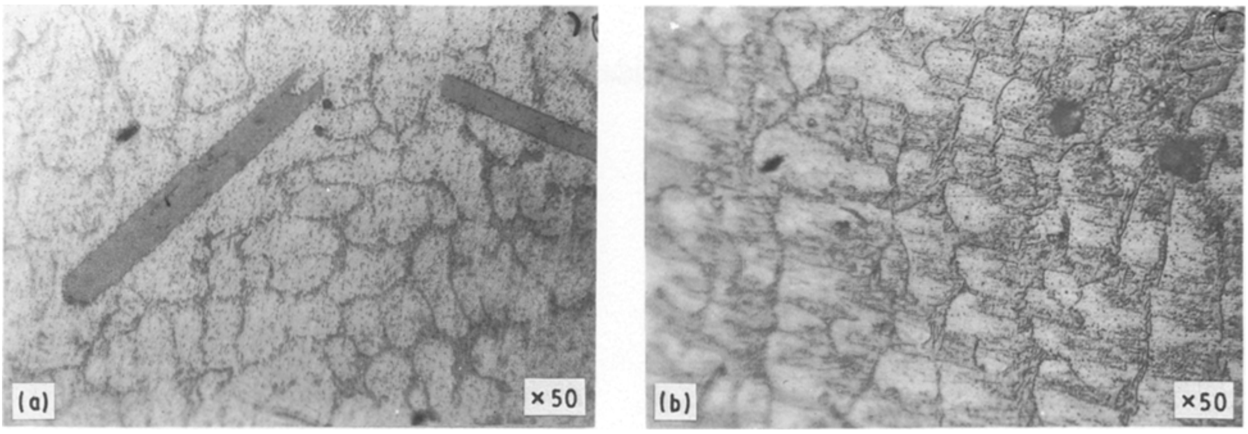

Figure 3 Optical micrograph of conventionally chill cast (a) Al–6Fe and (b) Al–6Fe–3MM.

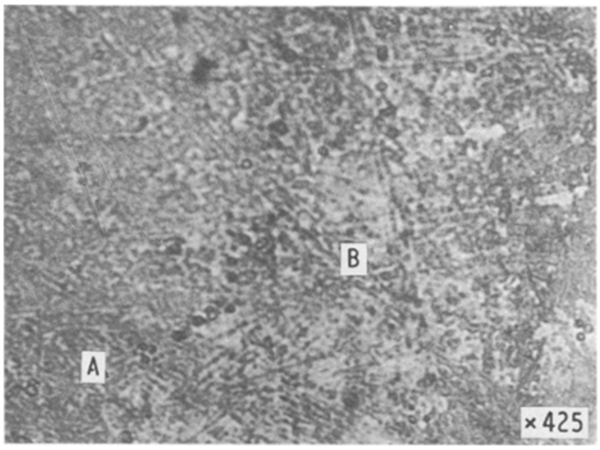

Figure 4 Microstructure of Al–6Fe–3MM ribbon in the melt spun condition. Note A and B zones.

It may be pointed out that the Zone A structure is the type of structure desired in high temperature alloys because of the fine grain size and the ribbon technique appears to be a viable process for getting the desired structure in suitably designed alloy systems [14].

The microstructures of the as extruded-forged-hot rolled sheet (Fig. 5) and the structures after heat treatment at 200 and 300 °C for 1 h and 3.5 h (Fig. 6) reveal that the fine and coarse structures remain unchanged. This indicates that diffusion of Fe has not taken place in the RS alloys.

3.1. TEM studies

Specimens 200–300 μm thick were cut from the short transverse section sheets of Al–6Fe–3MM alloy (extruded-forged-rolled) and thinned in a jet polishing machine using an electrolyte consisting of perchloric acid and ethyl alcohol. The specimens were examined using Philips EM-400 electron microscope operating at 120 kVA. Fig. 7 shows the microstructures of Zone A and Zone B, respectively. Average volume fraction of second phase particles in Zone B is much higher than in Zone A. The SAD of the second phase revealed that they are $FeAl_3$ in both the zones.

The above Al–6Fe–3MM rapidly solidified and processed sheets were given a solution treatment at 460 °C for 1 h and aged at 180 °C for 4 h. Transmission electron microscope (TEM) studies under this condition showed nucleation of $FeAl_3$ precipitates at dislocations (Fig. 8) and grain boundary junctions.

The as melt spun ribbon under the TEM showed the presence of Al_8Fe_4Ce compounds in grain boundaries and grain boundary junctions and these were spherical in shape.

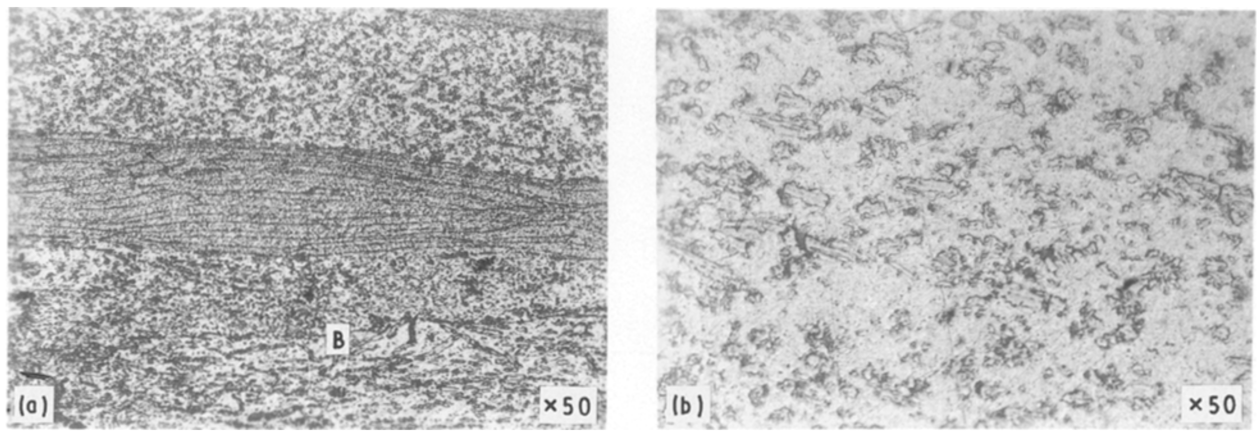

Figure 5 Microstructure of RSP sheet of Al–6Fe–3MM (hot rolled). Notice distinct bands of fine A and coarse B regions in (a). B region is enlarged in (b).

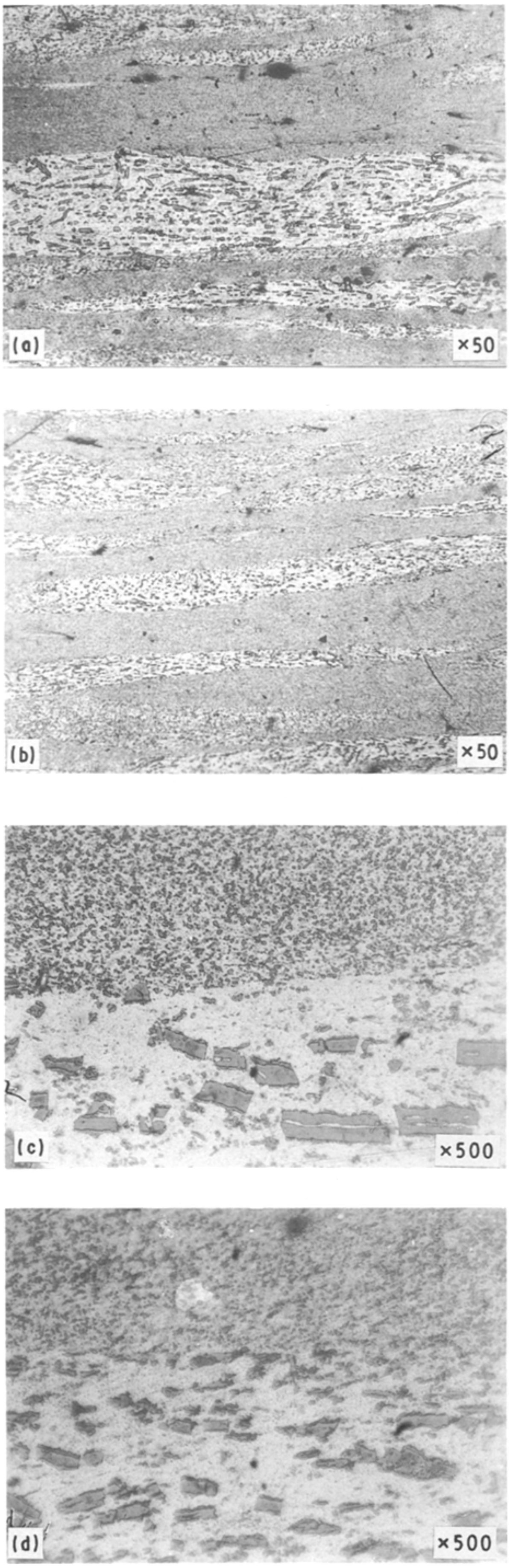

Figure 6 Microstructures of Al–6Fe–3MM RSP hot rolled sheet after heat treatment: (a) 300 °C/1 h, (b) 300 °C/3.5 h, (c) 200 °C/1 h, and (d) 200 °C/3.5 h.

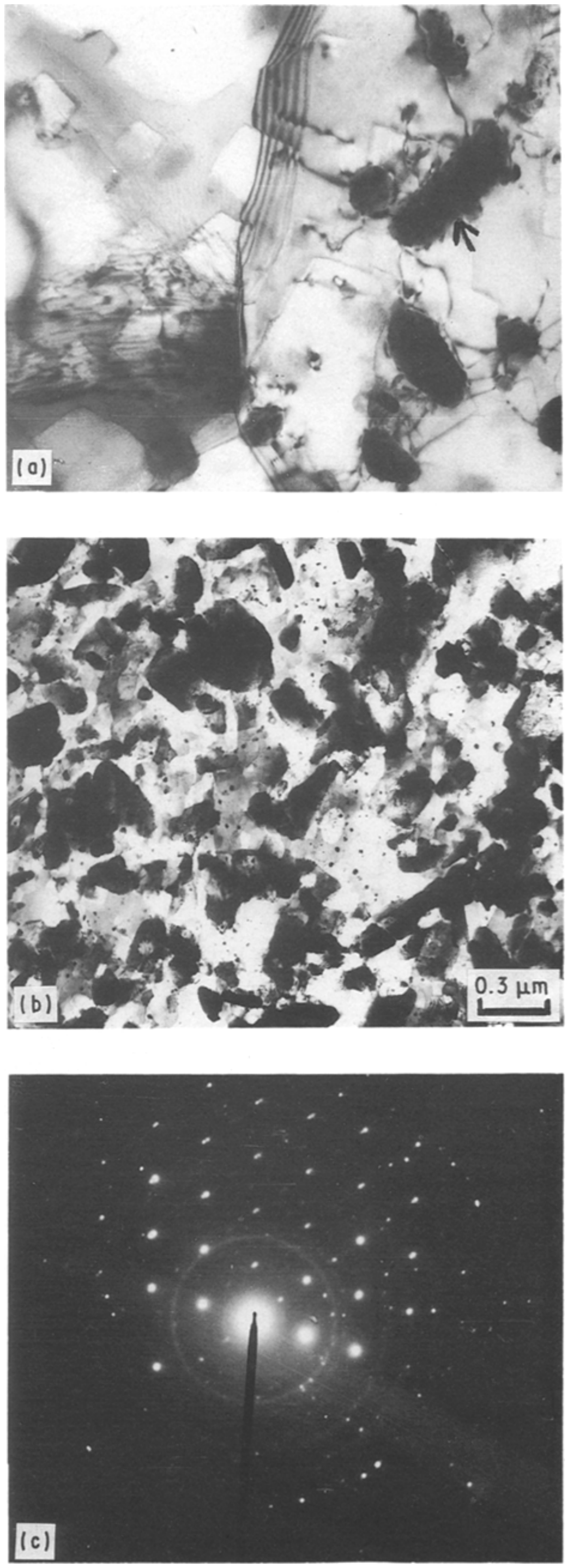

Figure 7 TEM photographs (a) and (b) showing microstructures of RSP Al–6Fe–3MM and SAD (c) of the second phase particles. The faint rings in (c) are from (1 1 0), (2 0 0) and (2 2 0) planes of aluminium matrix. The spots are from particles ($FeAl_3$) marked with an arrow in (a). Zone axis (0 1 0).

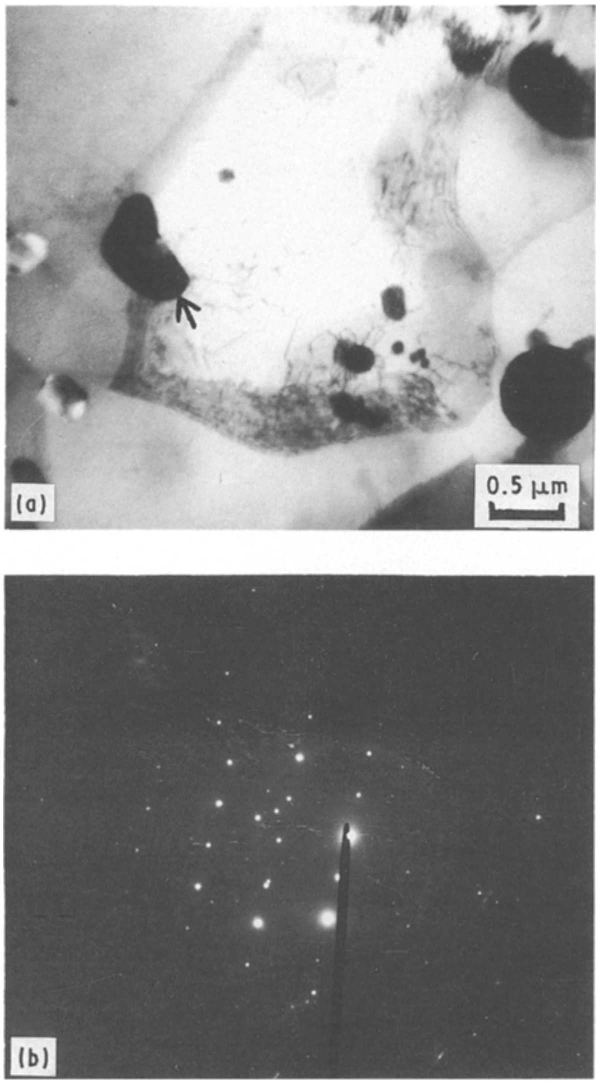

Figure 8 TEM photographs of RSP Al–6Fe–3MM sheet (hot rolled), solution treated at 460 °C for 1 h and water quenched followed by ageing at 180 °C for 4 h. (b) SAD from the second phase particle, Al_8CeFe_4.

TABLE IV XRD data of RS Al–6Fe–3MM

RS Ribbon		RSP Sheet	
d (pm)	Phases identified	*d* (pm)	Phases identified
303.86	Al_8CeFe_4, $FeAl_6$	404.17	$FeAl_3$
234.05	Al	395.54	$FeAl_3$
209.48	$FeAl_3$	368.27	$FeAl_3$
202.64	Al	353.89	$FeAl_3$
187.57	Al_8CeFe_4, $FeAl_6$	326.41	$FeAl_3$
143.22	Al	256.58	Al_8CeFe_4
122.13	Al	251.68	Al_8CeFe_4
116.94	Al	233.64	Al
		222.33	$FeAl_3$
		209.63	$FeAl_3$
		204.66	Al_8CeFe_4
		202.33	Al
		143.15	Al
		134.11	$FeAl_6$
		122.11	Al
		121.96	$FeAl_6$
		116.93	Al

3.2. X-Ray diffraction analysis

X-ray diffraction data of RS and RSP Al–6Fe–3MM specimens are given in Table IV. It is evident that the RS ribbons as well as RSP (extruded-forged-rolled) material show presence of Al_8CeFe_4, $FeAl_6$ and $FeAl_3$, the latter being predominant as second phase particles. The presence of these intermetallics in the RS ribbon both on chill side and air side has also been seen under optical microscope and the electron microscope. The presence of intermetallics on the chill side could be attributed to the fact that the intermetallics present in the solid state prior to melting did not go into solution on melting for melting spinning.

4. Conclusions

It has been shown in the present work that RS Al–6Fe–3MM ribbon exhibit a Zone A with relatively low volume fraction of second phase particles near the chill side and a Zone B consisting of a large volume fraction of coarse particles towards the air side. These zones persist in rapidly solidified and processed (RSP) sheets through cold consolidation hot extrusion, forging and rolling. The second phase particles in Zone A and Zone B were found to be $FeAl_3$ and Al_8CeFe_4 in the RSP heat treated sheet. Al_6Fe was also indicated in addition to these phases in as cast ribbon.

Acknowledgements

The authors wish to record their thanks to Dr O. N. Mohanty, Deputy Director and to the Director, National Metallurgical Laboratory for their encouragement in this work. They also wish to thank the TEM group headed by Dr A. Ghose for the electron microscopy work.

References

1. B. H. KEAR and M. COHEN (eds), "Rapid Solidification Processing: Principles and Techniques" (Claitor's Publishing Division, Baton Range LA, 1980).
2. R. RAY, in Proceedings of the 4th International Conference of Rapidly Quenched Metals, edited by T. Masumoto and K. Suzuki (The Japan Institute of Metals, 1982) p. 1515.
3. S. C. LANGENBECK and R. A. RAIMEN, AFWAL-TR-86–4027 (1986).
4. C. M. ADAMS, in "Rapidly Solidified Amorphous and Crystalline Alloys", edited by B. H. Kear, B. C. Giessen and M. Cohen (Elsevier, New York, 1982) p. 411.
5. T. R. ANANTHARAMAN, Proceedings of the Aluminium Congress II, January 1987 (Delhi, India) p. 1.
6. C. JANSAN, Splat Cooled Al-Rich Transition Metal Alloys, (PhD Thesis, MIT, August 1971).
7. S. K. DAS, K. OKAZAKI and C. M. ADAMS, in Proceedings of High Temperature Alloys: Theory and Design, edited by J. O. Stiegler, 9–11 April 1984, p. 451.
8. S. K. DAS, Proceedings of the International Conference on Rapid Solidification Processing & Technology ICMS-89, edited by C. S. Sivaramakrishnan and O. N. Mohanty, 15–17 March 1989, India.
9. H. JONES, *Mater. Sci. Eng.* **5** (1969/1970) 1.
10. H. L. FRASER, RSP and Powder Metallurgy of Aluminium Alloys, Second Annual Report, AFOSR Grant No. 82-D186, October 1986.
11. J. W. JINDEL, J. T. STANLEY, R. D. FIELD and H. L. FRASER, ASM Symposium Rapidly Solidified Powder Alluminium Alloys, 4–5 September 1984.

12. J. M. SATER, S. C. JHA and T. H. SANDERS, *Mater Sci. Eng.* **91** (1987) 201.
13. H. A. DAVIES, N. SHOHOJI and D. H. WARRINGTON, Proceedings of the 2nd International Conference on Rapid Solidification Processing: Principles and Techniques Reston VA, 23–26 March, 1980 (Claitor's Publishing Division, Baton Range LA, 1980) p. 153.
14. L. ACKERMANN, S. DERMARKAR and J. F. FAURE, "Aluminium Technology 86", edited by T. Sheppard (Institute of Metals, 1986) p. 698.

Received 9 March
and accepted 3 December 1990